Journal of Alloys and Compounds 509 (2011) 1197–1200

Contents lists available at ScienceDirect

Journal of Alloys and Compounds

journal homepage: www.elsevier.com/locate/jallcom

Preparation and luminescent characteristics of $Sr_3RE_2(BO_3)_4$:Dy^{3+} (RE = Y, La, Gd) phosphors for white LED

Zhang Rui, Wang Xiang*

Materials Science and Chemical Engineering College, Tianjin Polytechnic Univerisity, Hedong District, Tianjin, China

ARTICLE INFO

Article history:
Received 18 March 2010
Received in revised form
25 September 2010
Accepted 28 September 2010
Available online 8 October 2010

Keywords:
Luminescence
White-light-emitting phosphors
$Sr_3RE_2(BO_3)_4$:Dy^{3+} (RE = Y
La
Gd)
UV-LED

ABSTRACT

Dysprosium-activated $Sr_3RE_2(BO_3)_4$ (RE = Y, La, Gd) phosphors were synthesized by a high temperature solid-state reaction method. The phase uniformity of the phosphors was characterized by X-ray powder diffraction (XRD) and the luminescence characteristics were investigated. The excitation spectra at 575 nm emission show strong spectral bands in the region of 300–500 nm. The emission spectra of the phosphors with 365 nm excitation show three bands centered at 484 nm, 575 nm and 680 nm, which originate from the transitions of $^4F_{9/2} \rightarrow {}^6H_{15/2}$, $^4F_{9/2} \rightarrow {}^6H_{13/2}$ and $^4F_{9/2} \rightarrow {}^6H_{11/2}$ of Dy^{3+}, respectively. The effect of Dy^{3+} concentration on the emission intensity of the phosphors was investigated. The fluorescence decay curves for $^4F_{9/2} \rightarrow {}^6H_{13/2}$ excited at 365 nm and monitored at λ_{em} of 575 nm were measured. The decay times decreased slowly with increasing Dy^{3+} doping concentration due to a trap capturing to resonance fluorescence transfer of the activated ions and due to the exchange interactions between activated ion pairs. In order to determine the type of interaction between activated ions, the concentration dependence curves ($\lg(I/x)$ versus $\lg x$) of $Sr_3RE_2(BO_3)_4$:Dy^{3+} (RE = Y, La, Gd) were plotted. The concentration quenching mechanism of the $^4F_{9/2} \rightarrow {}^6H_{13/2}$ (575 nm) transition of Dy^{3+} is the d–d interaction. All results indicate these phosphors are promising white-color luminescent materials.

1. Introduction

In recent years, the common way to fabricate white light emitting diodes (W-LED) is to use a blue-emitting GaN chip to pump a YAG:Ce^{3+} phosphor or an ultraviolet InGaN chip to excite blue-, green-, and red-emitting multiphase phosphors [1,2]. However, there are some drawbacks to these combinations, for example, white-emitting color changes with input powder and temperature, low color rendering index and low color reproducibility [3,4]. In addition, W-LEDs are fabricated by using two or three different kinds of phosphors and reabsorption of emission wavelengths leads to a decrease in luminous efficiency [5]. Therefore, in order to solve these problems, it is essential to exploit single-phased full-color-emitting phosphors for UV-pumped white LED [6]. At present, single-phased white light emitting phosphors are receiving a great deal of attention [7–9]. Among these phosphors investigated, borates are good candidates due to their low synthetic temperatures, stabilities, and low costs [10].

The hosts $Sr_3Y_2(BO_3)_4$ has orthorhombic structure with a *Pc*21*n* space group. The structure of $Sr_3Y_2(BO_3)_4$ is formed by isolated BO_3 triangles, strontium–oxygen polyhedra, and Y–oxygen polyhedra. The trivalent rare-earth ions occupy two different crystallographic sites and each has an eightfold coordination to form YO_8 polyhedra [11,12]. The structure information for $Sr_3Y_2(BO_3)_4$ indicates that the longer distance between the rare-earth ions maybe accommodate higher doping concentration.

Dysprosium ion with a $4f^9$ configuration has complicated f-block energy levels and between these levels various transitions result in sharp line spectra [13–15]. Dy^{3+} ion exhibits three visible emission bands including a blue emission at 484 nm, corresponding to the $^4F_{9/2} \rightarrow {}^6H_{15/2}$ transition, a yellow emission at 575 nm, corresponding to the hypersensitive transition $^4F_{9/2} \rightarrow {}^6H_{13/2}$ ($\Delta L = 2$; $\Delta J = 2$), and a weak red emission at 665 nm, corresponding to the $^4F_{9/2} \rightarrow {}^6H_{11/2}$ transition. Thus $Sr_3RE_2(BO_3)_4$:Dy^{3+} (RE = Y, La, Gd) should be useful as a single-phased full-color-emitting phosphor for UV-pumped white LED.

Li et al. reported the preparation and luminescent properties of $Sr_3Y_2(BO_3)_4$:Dy^{3+} [16]. However, to our knowledge, little detailed information is available on luminescent properties of borate-based phosphors $Sr_3RE_2(BO_3)_4$:Dy^{3+} (RE = Y, La, Gd), especially the concentration quenching mechanism of Dy^{3+}. In this paper, $Sr_3RE_2(BO_3)_4$:Dy^{3+} (RE = Y, La, Gd) phosphors were prepared by a high temperature solid-state reaction method and a detailed study was carried out on the luminescence properties of the phosphors and the concentration quenching mechanism of Dy^{3+}.

* Corresponding author. Tel.: +86 13207573812; fax: +86 22 26323731.
E-mail address: wangxiangzr@163.com (X. Wang).

0925-8388/$ – see front matter.
doi:10.1016/j.jallcom.2010.09.177

2. Experimental

Dy_2O_3 (99.99%), Y_2O_3 (99.99%), La_2O_3 (99.99%), Gd_2O_3 (99.99%), $SrCO_3$ (99.0%), H_3BO_3 (99.5%) and ethanol (99%) were used as starting materials. $Sr_3Y_2(BO_3)_4$:Dy^{3+} were synthesized by a high temperature solid-state reaction method in air. The chemical equation for the reaction is:

$$3SrCO_3 + 4H_3BO_3 + (1-x/2)Y_2O_3 + x/2Dy_2O_3 = Sr_3Y_{2-x}(BO_3)_4{:}\ Dy_x^{3+} + 3CO_2 + 6H_2O$$

Stoichiometric amount of starting materials were mixed thoroughly by using ethanol as medium for a homogeneous mixing in an agate mortar. The homogeneous mixture was then transferred into an alumina crucible and heated at 1250 °C for 2 h. Other samples using La_2O_3 or Gd_2O_3 instead of Y_2O_3 were synthesized by the same process.

The phase purity and phase structure of the powder samples were characterized by X-ray powder diffraction spectroscopy (XRD), using a BDX 3300 X-ray diffractometer with Ni-filtered CuKα radiation at 30 kV and 20 mA. A scan rate of 8°/min was applied to record the patterns in the 2θ range of 10–70°.

Excitation and emission spectra of Dy^{3+}-activated $Sr_3RE_2(BO_3)_4$ (RE = Y, La, Gd) phosphors at room temperature were determined with RF-5301 fluorophotometer

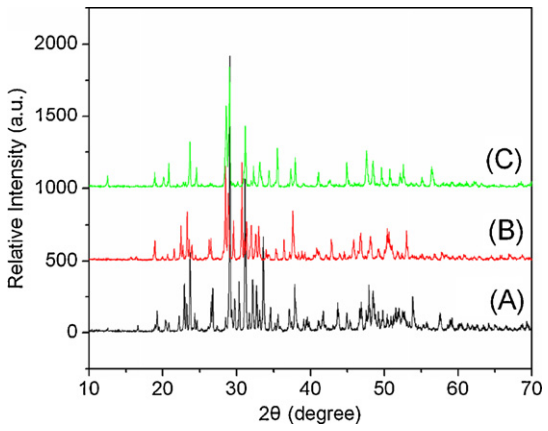

Fig. 1. The XRD patterns of $Sr_3Y_2(BO_3)_4$:Dy^{3+} (A), $Sr_3La_2(BO_3)_4$:Dy^{3+} (B), and $Sr_3Gd_2(BO_3)_4$:Dy^{3+} (C) phosphors.

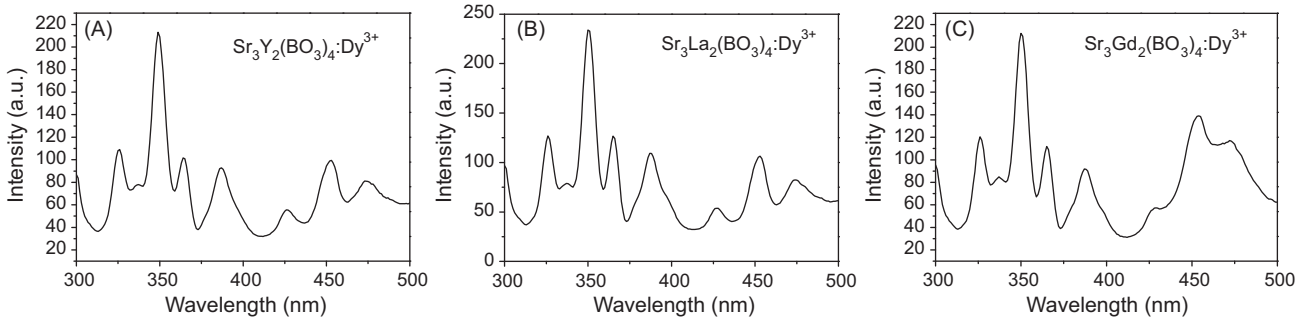

Fig. 2. Excitation spectra of $Sr_3Y_2(BO_3)_4$:Dy^{3+} (A), $Sr_3La_2(BO_3)_4$:Dy^{3+} (B), and $Sr_3Gd_2(BO_3)_4$:Dy^{3+} (C) phosphors at 575 nm emission.

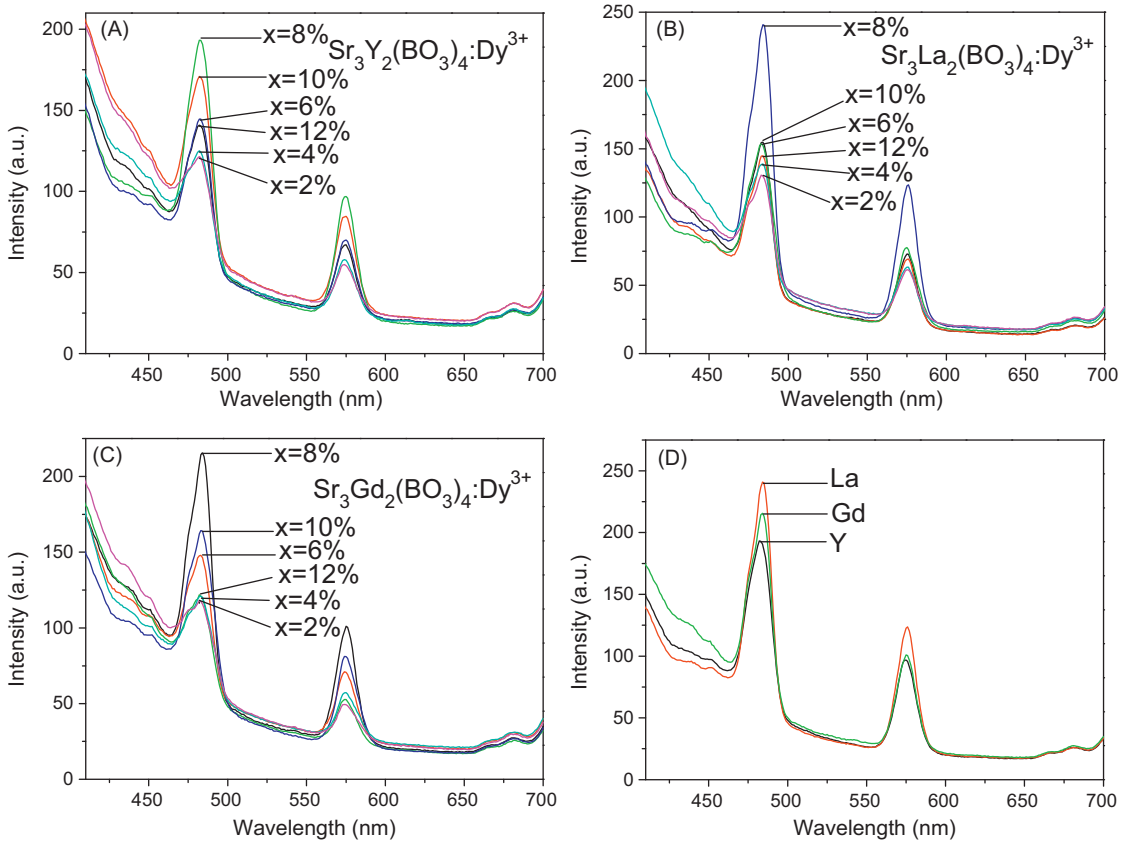

Fig. 3. Emission spectra of $Sr_3Y_2(BO_3)_4$:Dy^{3+} (A), $Sr_3La_2(BO_3)_4$:Dy^{3+} (B), and $Sr_3Gd_2(BO_3)_4$:Dy^{3+} (C) phosphors with 365 nm excitation at different doping concentration, and emission spectra for the three above phosphors each containing the same amount of doped Dy^{3+} (8 mol%) (D).

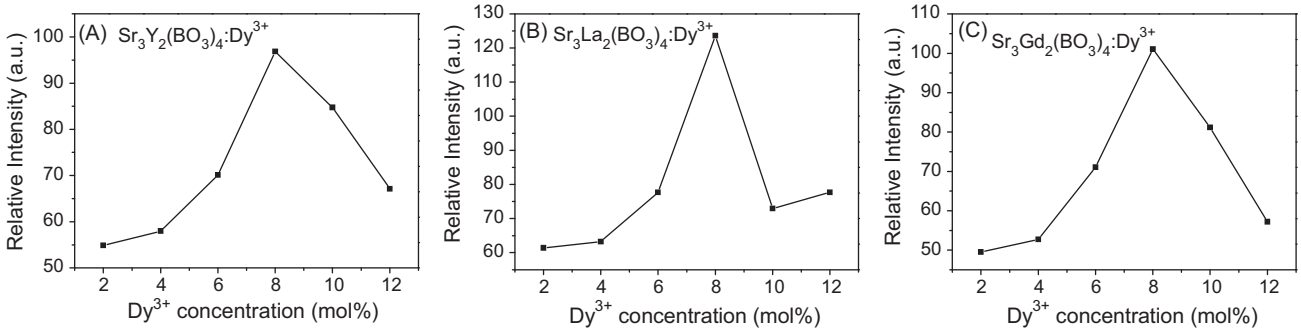

Fig. 4. The dependence of the 575 nm emission intensity of $Sr_3Y_2(BO_3)_4:Dy^{3+}$ (A), $Sr_3La_2(BO_3)_4:Dy^{3+}$ (B), and $Sr_3Gd_2(BO_3)_4:Dy^{3+}$ (C) phosphors on Dy^{3+} concentration.

with a 450-W xenon lamp as the excitation source. The luminescence decay curves were obtained with a Lecroy Wave Runner 6100 Digital Oscilloscope (1 GHz) using a tunable laser (pulse width = 4 ns, gate = 50 ns) as the excitation source (Contimuum Sunlite OPO).

3. Results and discussion

Polycrystalline samples of $Sr_3Y_2(BO_3)_4:Dy^{3+}$, $Sr_3La_2(BO_3)_4:Dy^{3+}$, and $Sr_3Gd_2(BO_3)_4:Dy^{3+}$ phosphors were obtained as described above. The XRD patterns for these samples with 8mol% Dy^{3+} are presented in Fig. 1. All the prepared samples have the similar XRD patterns and show similar crystalline structure. It is well known that rare earth ions have similar radius, coordination structure and physical–chemical properties. When RE^{3+} (RE = Y, La, Gd) is replaced by Dy^{3+}, the crystal structure does not change dramatically [16,17]. For example, the XRD pattern for $Sr_3Y_2(BO_3)_4:Dy^{3+}$ is consistent with XRD patterns reported in literature [16]. Most of the peaks can be assigned to the $Sr_3Y_2(BO_3)_4$ phase. The cell parameters of $Sr_3Y_2(BO_3)_4$ are $a = 0.87$ nm, $b = 1.60$ nm, and $c = 0.74$ nm (DICVOL91 program). The $Sr_3Y_2(BO_3)_4$ is in an orthorhombic phase with a $Pc21n$ space group, which indicates that the Dy^{3+} ion has replaced the site of Y^{3+} ions in this host. In other words, the doping with Dy^{3+} ions does not form new phases during the synthesis.The Dy^{3+} ions have entered the host lattice of $Sr_3Y_2(BO_3)_4$ and do not change the crystal structure. The same is true for $Sr_3La_2(BO_3)_4:Dy^{3+}$ and $Sr_3Gd_2(BO_3)_4:Dy^{3+}$ structures.

The excitation spectra of the $Sr_3RE_2(BO_3)_4:Dy^{3+}$ (RE = Y, La, Gd) phosphors monitored at 575 nm are shown in Fig. 2. All the excitation spectra show similar features, so $Sr_3Y_2(BO_3)_4:Dy^{3+}$ will be used for discussion purposes. There are some sharp absorption peaks in wavelength region of 300–500 nm, which are due to excitation of the f–f shell transitions of Dy^{3+} [15]. The several band peaks at 326 nm, 350 nm, 365 nm, 387 nm, 426 nm, 453 nm and 473 nm correspond to the transitions from the ground state $^6H_{15/2}$ to the excited states $^4K_{15/2}$; $^4P_{7/2}$; $^4P_{3/2}$; $^4F_{7/2}$; $^4G_{21/2}$; $^4H_{15/2}$; and $^6F_{9/2}$, respectively, and the maximum excitation wavelength is located at 350 nm [15,16,18].

Fig. 3 shows the emission spectra of the $Sr_3RE_2(BO_3)_4:Dy^{3+}$ (RE = Y, La, Gd) phosphors with 365 nm excitation [$Sr_3Y_2(BO_3)_4:Dy^{3+}$ (A); $Sr_3La_2(BO_3)_4:Dy^{3+}$ (B); $Sr_3Gd_2(BO_3)_4:Dy^{3+}$ (C), respectively]. The emission spectra were measured in the range of 410–700 nm. Again, all three emission spectra show similar features, $Sr_3Y_2(BO_3)_4:Dy^{3+}$ will be discussed as representative. Three emission bands peaked at 484 nm, 575 nm and 680 nm are observed. The blue emission at 484 nm is related to $^4F_{9/2} \rightarrow {}^6H_{15/2}$ magnetic dipole transition, the yellow emission at 575 nm is ascribed to $^4F_{9/2} \rightarrow {}^6H_{13/2}$ electric dipole transition, and the weak red band peaked at 680 nm corresponds to the $^4F_{9/2} \rightarrow {}^6H_{11/2}$ transition [19,20]. Within these emission transitions, the yellow band and the blue band are the predominant transitions. The $^4F_{9/2} \rightarrow {}^6H_{13/2}$ transition is hypersensitive ($\Delta L = 2$; $\Delta J = 2$), and it can be influenced by its microscopic environment so its intensity strongly depends on the host, but the intensity of the $^4F_{9/2} \rightarrow {}^6H_{15/2}$ transition is less sensitive to the host. The spectra and peak assignments for $Sr_3La_2(BO_3)_4:Dy^{3+}$ (Fig. 3B) and $Sr_3Gd_2(BO_3)_4:Dy^{3+}$ (Fig. 3C) are similar to $Sr_3Y_2(BO_3)_4:Dy^{3+}$.

The emission intensities for the three phosphors with a Dy^{3+} doping concentration of 8 mol% were compared and the results are shown in Fig. 3D. The $La_2(BO_3)_4:Dy^{3+}$ has the highest intensity at 575 nm and the $Sr_3Y_2(BO_3)_4:Dy^{3+}$ has the lowest.

The effect of the Dy^{3+} concentration on the emission intensity of the $^4F_{9/2} \rightarrow {}^6H_{13/2}$ (575 nm) transition with 365 nm excitation is shown in Fig. 4. Here again all the three graphs show similar trends and it is obvious that the luminescent intensities of all three phosphors are strongly affected by the ratio of doped Dy^{3+} (2, 4, 6, 8, 10, or 12 mol%). The emission intensities increased rapidly with increasing Dy^{3+} concentration until the concentration reached 8 mol%. At concentrations above 8 mol% the intensities decreased. In other words, when the Dy^{3+} concentration was 8 mol%, the $Sr_3RE_2(BO_3)_4:Dy^{3+}$ (RE = Y, La, Gd) phosphors exhibit the highest emission for the $^4F_{9/2} \rightarrow {}^6H_{13/2}$ (575 nm) transition.

In order to analyze on the mechanism of concentration quenching, the fluorescence decay curves for $Sr_3Gd_2(BO_3)_4:xDy^{3+}$ were measured. Fig. 5 shows the fluorescence decay curves for $^4F_{9/2} \rightarrow {}^6H_{13/2}$ excited at 365 nm and monitored at 575 nm. The results indicate that the presence of Dy^{3+} produces weak quenching in the $Sr_3Gd_2(BO_3)_4:xDy^{3+}$ phosphors even at low doping concentrations. Each of the five decay patterns consists of a fast decay and a subsequent slow decay with a long decay tail. The initial intensities of the fast component in the $Sr_3Gd_2(BO_3)_4:xDy^{3+}$ phosphors are affected by the ratio of Dy^{3+} doping. The initial intensity increases

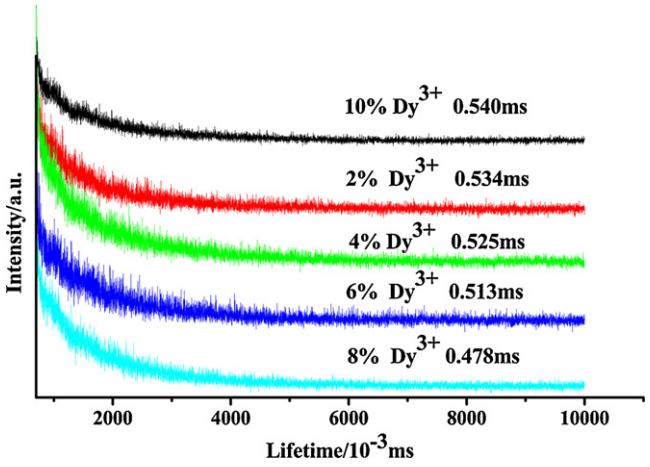

Fig. 5. The decay curves of the phosphorescence at 575 nm in $Sr_3Gd_2(BO_3)_4:xDy^{3+}$ after UV excitation at 365 nm.

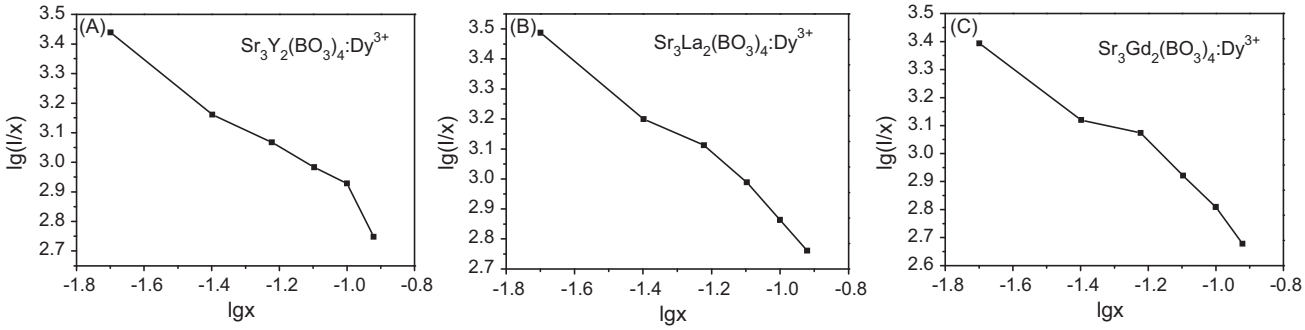

Fig. 6. Relationship between the lg(I/x) and lg x of Dy^{3+} for $Sr_3Y_2(BO_3)_4:Dy^{3+}$ (A), $Sr_3La_2(BO_3)_4:Dy^{3+}$ (B), and $Sr_3Gd_2(BO_3)_4:Dy^{3+}$ (C) phosphors (λ_{ex} = 365 nm).

with increasing Dy^{3+} concentration until 8 mol% is reached and then at higher Dy^{3+} concentrations the initial intensity decreases.

The fast decay component of the fluorescence decay curves for $Sr_3Gd_2(BO_3)_4:xDy^{3+}$ was fitted using a single exponential formula and the decay time is on the order of microseconds. As indicated in Fig. 5, the decay times of Dy^{3+} ions were determined to be 534, 525, 513, 478 and 540 μs for $Sr_3Gd_2(BO_3)_4:xDy^{3+}$ with x = 0.02, 0.04, 0.06, 0.08 and 0.10, respectively. The decay times decrease slowly with increasing Dy^{3+} doping concentrations up to 8%. This can be attributed to two reasons. The first is that with increasing concentrations of doped ions, the activated ions density around the quenching center is increased, which can result in a trap capture to resonance fluorescence transfer of the activated ions [21]. The other reason is that the exchange interactions between activated ions pairs results in the shorter decay times as the concentration of activated ions increases as proposed by Ronda and Amrein [22].

However, for $Sr_3Gd_2(BO_3)_4:xDy^{3+}$ when x = 0.10, the phosphor has a smaller luminescent intensity but a longer decay time. This result suggests the decrease of luminescent intensity for $Sr_3Gd_2(BO_3)_4:xDy^{3+}$ phosphors with higher Dy^{3+} concentration can not simply be attributed to concentration quenching. It may be that the fluorescence capturing effect is stronger in higher Dy^{3+} doped phosphors and thus concentration quenching is enhanced.

In order to determine the type of interaction between activated ions, the $Sr_3RE_2(BO_3)_4:Dy^{3+}$ (RE = Y, La, Gd) phosphors were excited at 365 nm and the emission intensities (I) of the $^4F_{9/2} \rightarrow {}^6H_{13/2}$ (575 nm) transition were measured. Concentration dependence curves of lg(I/x) versus lg x were then plotted and are shown in Fig. 6. The slopes of the linear section of the concentration quenching curves are −1.33, −1.29, −1.38 for $Sr_3Y_2(BO_3)_4:Dy^{3+}$, $Sr_3La_2(BO_3)_4:Dy^{3+}$ and $Sr_3Gd_2(BO_3)_4:Dy^{3+}$, respectively. They are all located in [−2,−1]. According to the theory of Huang and Lou [23], the concentration quenching mechanism of the $^4F_{9/2} \rightarrow {}^6H_{13/2}$ (575 nm) transition of Dy^{3+} in $Sr_3RE_2(BO_3)_4$ (RE = Y, La, Gd) is the d–d interaction. This result is in agreement with Dexter's theory [24].

4. Conclusions

In conclusion, phosphors of $Sr_3RE_2(BO_3)_4$ (RE = Y, La, Gd) doped with Dy^{3+} ion were designed and successfully synthesized by a high temperature solid-state reaction method. The excitation spectra at 575 nm emission have several bands in the region of 300–500 nm, which are coupled well with the emission of UV LED (350–410 nm) and blue LED (450–470 nm). Under 365 nm excitation, three emission bands centered at 484 nm, 575 nm and 680 nm are observed and they correspond to the transitions of $^4F_{9/2} \rightarrow {}^6H_{15/2}$, $^4F_{9/2} \rightarrow {}^6H_{13/2}$, and $^4F_{9/2} \rightarrow {}^6H_{11/2}$ of Dy^{3+}, respectively. The emission intensity of the 575 nm emission increases rapidly with increasing Dy^{3+} concentration up to 8 mol%. When the Dy^{3+} concentration is above 8 mol% concentration quenching occurs. The fluorescence decay curves for $^4F_{9/2} \rightarrow {}^6H_{13/2}$ excited at 365 nm and monitored at 575 nm were measured. The decay times decrease slowly with increasing Dy^{3+} doping concentration due to trap capturing to resonance fluorescence transfer of the activated ions and due to the exchange interactions between activated ion pairs. In order to determine the type of interaction between activated ions, the concentration dependence curves (lg(I/x) versus lg x) of $Sr_3RE_2(BO_3)_4$ (RE = Y, La, Gd) were plotted. The concentration quenching mechanism of the $^4F_{9/2} \rightarrow {}^6H_{13/2}$ (575 nm) transition of Dy^{3+} is a d–d interaction. All of these results show that $Sr_3RE_2(BO_3)_4:Dy^{3+}$ (RE = Y, La, Gd) are promising full-color-emitting phosphors for UV-pumped w-LED.

Acknowledgements

This work was supported by the Tianjin Technology Development Foundation (Grant No. 06YFGPGX07700).

References

[1] Z.L. Wang, H.B. Liang, M.L. Gong, Q. Su, Opt. Mater. 29 (2007) 896–900.
[2] J.S. Kim, P.E. Jeon, J.C. Choi, H.L. Park, S.I. Mho, G.C. Kim, Appl. Phys. Lett. 84 (2004) 2931–2933.
[3] L. Zhou, J. Wei, J. Wu, F. Gong, L. Yi, J. Huang, J. Alloys Compd. 476 (2009) 390–392.
[4] C.F. Guo, Y. Xu, F. Lv, X. Ding, J. Alloys Compd. 497 (2010) L21–L24.
[5] J.S. Kim, J.Y. Kang, P.E. Jeon, J.C. Chol, H.L. Park, T.W. Kim, Jpn. J. Appl. Phys. Part 1 43 (2004) 989–992.
[6] W.B. Ma, Z.P. Shi, R. Wang, J. Alloys Compd. 503 (2010) 118–121.
[7] X.D. Qi, C.M. Liu, C.C. Kuo, J. Alloys Compd. 492 (2010) L61–L63.
[8] B.V. Rao, K. Jang, H.S. Lee, S.S. Yi, J.H. Jeong, J. Alloys Compd. 496 (2010) 251–255.
[9] K.H. Kwon, W.B. Im, H.S. Jang, H.S. Yoo, D.Y. Jeon, Inorg. Chem. 48 (2009) 11525–11529.
[10] T.-W. Kuo, T.-M. Chen, J. Lumin. 130 (2010) 483–487.
[11] Y. Zhang, L. Yadong, J. Alloys Compd. 384 (2004) 88–92.
[12] L. He, Y.H. Wang, J. Alloys Compd. 431 (2007) 226–229.
[13] Q. Su, Z.W. Pei, J. Lin, F. Xue, J. Alloys Compd. 225 (1995) 103–108.
[14] T.R.N. Kutty, Mater. Res. Bull. 25 (1990) 485–490.
[15] B. Yan, C. Wang, J. Alloys Compd. 462 (2008) 147–152.
[16] P.L. Li, Z.P. Yang, Z.J. Wang, Q.L. Guo, Mater. Lett. 62 (2008) 1455–1457.
[17] R.P. Rao, D.J. Devine, J. Lumin. 87 (2000) 1260–1263.
[18] C.H. Yang, Y.X. Pan, Q.Y. Zhang, Mater. Sci. Eng. B 137 (2007) 195–199.
[19] C.H. Yang, Y.X. Pan, Q.Y. Zhang, Chin. Rare Metal Mater. Eng. 37 (2008) 568–574.
[20] B. Yan, X.Q. Zhang, H.S. Lai, Chin. J. Lumin. 28 (2007) 531–534.
[21] E. Snoeks, P.G. Kik, Opt. Mater. 5 (1996) 159–167.
[22] C.R. Ronda, T. Amrein, J. Lumin. 69 (1996) 245248.
[23] S.H. Huang, L.R. Lou, Chin. J. Lumin. 11 (1) (1990) 1–4.
[24] D.L. Dexter, J. Chem. Phys. 22 (6) (1954) 1063–1069.